Biophysical Journal Volume 101 September 2011 1184–1192

On the Involvement of Single-Bond Rotation in the Primary Photochemistry of Photoactive Yellow Protein

Andreas D. Stahl,[†△] Marijke Hospes,[‡△] Kushagra Singhal,[‡] Ivo van Stokkum,[†] Rienk van Grondelle,[†] Marie Louise Groot,[†] and Klaas J. Hellingwerf[†‡*]

[†]Department of Physics and Astronomy, Faculty of Sciences, Vrije Universiteit Amsterdam, Amsterdam, The Netherlands; and [‡]Swammerdam Institute for Life Sciences, Science Faculty, University of Amsterdam, Amsterdam, The Netherlands

ABSTRACT Prior experimental observations, as well as theoretical considerations, have led to the proposal that C_4-C_7 single-bond rotation may play an important role in the primary photochemistry of photoactive yellow protein (PYP). We therefore synthesized an analog of this protein's 4-hydroxy-cinnamic acid chromophore, (5-hydroxy indan-(1E)-ylidene)acetic acid, in which rotation across the C_4-C_7 single bond has been locked with an ethane bridge, and we reconstituted the *apo* form of the wild-type protein and its R52A derivative with this chromophore analog. In PYP reconstituted with the rotation-locked chromophore, 1), absorption spectra of ground and intermediate states are slightly blue-shifted; 2), the quantum yield of photochemistry is ~60% reduced; 3), the excited-state dynamics of the chromophore are accelerated; and 4), dynamics of the thermal recovery reaction of the protein are accelerated. A significant finding was that the yield of the transient ground-state intermediate in the early phase of the photocycle was considerably higher in the rotation-locked samples than in the corresponding samples reconstituted with *p*-coumaric acid. In contrast to theoretical predictions, the initial photocycle dynamics of PYP were observed to be not affected by the charge of the amino acid residue at position 52, which was varied by 1), varying the pH of the sample between 5 and 10; and 2), site-directed mutagenesis to construct R52A. These results imply that C_4-C_7 single-bond rotation in PYP is not an alternative to C_7=C_8 double-bond rotation, in case the nearby positive charge of R52 is absent, but rather facilitates, presumably with a compensatory movement, the physiological Z/E isomerization of the blue-light-absorbing chromophore.

INTRODUCTION

In addition to reproduction, and its inherent errors, which are cornerstones of evolution, the ability to perceive environmental signals and adjust accordingly is a key characteristic of (cellular) life. It is therefore of prime importance to understand the molecular basis of the elementary steps of such signal transduction processes and when necessary to repair or improve these processes. Photosensory receptors, i.e., proteins that can generate a biological signal upon the absorption of a photon of visible electromagnetic radiation, have traditionally played a key role as model systems for such studies (1). The accuracy with which these proteins can be activated in time and space is unrivalled.

Several different families of these photosensory receptors have been characterized, each with their own specific (chromophore) structure and mechanism of primary photochemistry. Best known are the rhodopsins, in which the absorption of green light leads to Z/E isomerization of the retinal chromophore, and the LOV domains, which show blue-light-induced covalent adduct formation between the flavin chromophore and a nearby cysteine. Here, however, we have chosen yet another model system for such studies, photoactive yellow protein (PYP (2)), which functions as a photosensory receptor for a photophobic response in *Halorhodospira halophila* (3).

This protein displays an exceptional chemical and photochemical stability and has been characterized in detail with respect to structure and function, as discussed in previous work (4–6). PYP is a relatively small protein (125 amino acids), containing a 4-hydroxy cinnamic acid (or *p*-coumaric acid) chromophore, which is thiol-esterified to a cysteine residue, C69 of *apo*-PYP (7). The chromophore is buried inside the main hydrophobic core of this α/β-fold protein as a phenolate anion (8), stabilized by hydrogen bonding with E46 and Y42 (9) and in the *trans* configuration (10). It is significant that both hydrogen bonds show exceptional characteristics: they are very short and of the low-barrier and ionic-types, respectively (11).

Light absorption by the chromophore of PYP induces primary photochemistry in a photocycle that leads to its *cis* configuration within a few picoseconds (12), with a quantum yield of 0.35 (13,14). The structural transition underlying this Z/E isomerization can only be completed in a complex reaction, in which also the hydrogen bond between the C=O group of the chromophore and the nitrogen atom of the peptide bond between P68 and C69, is disrupted, after which the C=O group starts to rotate around the long axis of the chromophore to stabilize the isomerization of the C_7=C_8 ethylenic bond (15–17) to form the first *cis* ground-state intermediate (GSI), I_0, of this photocycle. In parallel, a transient GSI (18) is formed that also may have an isomerized C_7=C_8 ethylenic bond but has its carbonyl group still hydrogen-bonded to the nitrogen atom of the protein's backbone (19). This GSI

Submitted March 24, 2011, and accepted for publication June 17, 2011.

△Andreas D. Stahl and Marijke Hospes contributed equally to this work.

*Correspondence: K.J.Hellingwerf@uva.nl

Editor: Leonid S. Brown.

0006-3495/11/09/1184/9 $2.00

doi: 10.1016/j.bpj.2011.06.065

then rapidly (i.e., with a half-life of 6 ps) thermally relaxes back to the stable GSI.

The I_0 intermediate converts with ~100% efficiency to I_1 (also denoted pR_1), and subsequently to the pR_2 intermediate, presumably by additional configurational relaxation of the *cis* chromophore. Next, a proton is transferred from E46 to the chromophore (15,20) at a rate of ~10^3 s^{-1} to form the first of a series of blue-shifted intermediates (i.e., pB′) in this photocycle, which leads to (partial) unfolding of the protein (21) to form the signaling state pB. A complex thermal recovery process, which involves the pG′ intermediate, leads to re-formation of the ground state within 1 s (22–26).

Formation of the electronically excited singlet state through absorption of a blue photon is accompanied by a profound charge redistribution in the cinnamyl chromophore of PYP, as demonstrated with Stark spectroscopy (27). It is significant that in several polar organic dyes with a similar characteristic, based on a pronounced donor/acceptor asymmetry across their ethylenic bond, light absorption leads to the formation of a so-called twisted-intramolecular charge transfer (TICT) state (28). However, the structural transition that underlies formation of a TICT state may well be a rotation across a single rather than a C=C double bond (29), e.g., to position the π electron system of the tail of the coumaryl chromophore orthogonally with respect to those of its aromatic ring system (to which it is conjugated in the *trans* configuration).

The above described similarities have led to discussions as to whether or not single-bond rotation (e.g., around the C_4-C_7 bond) would be involved in the primary photochemistry of PYP as well. This issue became even more relevant when it was reported that quantum mechanics/molecular mechanics calculations on its primary photochemistry predicted that the positive charge of R52 is crucial to prevent the primary photochemistry of PYP from shifting from partial Z/E isomerization to single-bond isomerization only (17,30). However, experimental observations made on site-directed mutant derivatives of PYP in which R52 was replaced by a noncharged amino acid (31) have so far not provided indications for such a dramatic transition.

Nevertheless, there is yet another reason why this single-bond rotation could be relevant for the primary photochemistry of PYP: Besides the productive photochemistry of the protein, which leads to sequential formation of the photocycle intermediates I_0, I_1/pR, pB′, etc., a second GSI is formed in parallel to I_0 directly from the decay of the (manifold of) singlet excited state(s) (18,32). This intermediate has been characterized with both time-resolved ultraviolet-visible (UV-vis) and infrared spectroscopy (19), although the configuration of the chromophore in this GSI intermediate has not yet been conclusively resolved. Suggestions put forward range from a vibrationally hot ground state, via a *cis*-like intermediate, to a twisted phenolate intermediate.

Here, we address this issue by reconstituting apo-PYP with a chromophore analog in which rotation across the C_4-C_7 single bond was locked with an ethane bridge, thus creating a cyclopentane ring (see Fig. 1). For convenience, we refer to proteins reconstituted with this modified chromophore as rotation-locked. Furthermore, this modified chromophore was used not only in wild-type PYP but also in the R52A mutant, whereas the charge of R52 was also altered by varying the buffer pH. The primary photochemistry and subsequent photocycle transitions of these four proteins were then characterized with UV-vis transient absorption spectroscopy in the time domain ranging from picoseconds to seconds.

The results obtained reveal that neither the net charge of R52 nor C_4-C_7 single-bond rotation is critically required for the primary photochemistry of PYP. Nevertheless, rotational flexibility of the C_4-C_7 bond does contribute to an increase in the quantum yield of signaling state formation in PYP: restriction of this flexibility decreases the quantum yield of product formation in PYP and dramatically increases the yield of the GSI.

MATERIALS AND METHODS

Set-up for ultrafast visible spectroscopy

The ultrafast transient absorption experiments in the visible spectral range were performed with a setup described in more detail in Groot et al. (33). Briefly, the output of a Ti:Sapphire regenerative-amplified laser system operating at 1 kHz (Hurricane; SpectraPhysics, Mountain View, CA) is divided into two beams. One beam is sent to a BBO crystal to generate the excitation pulse at the desired center wavelength of 400 nm by

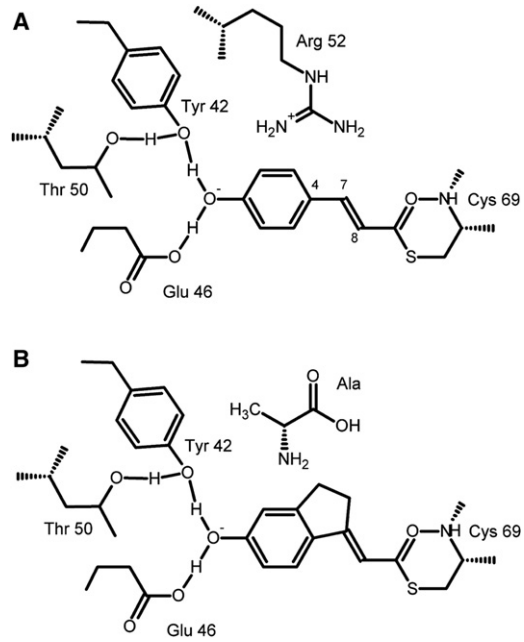

FIGURE 1 Schematic representation of the structure of the chromophore binding pocket of wild-type PYP before (*A*) and after (*B*) the two modifications characterized in this study, namely, the R52A mutation and replacement of the coumaryl chromophore by a rotation-locked derivative, (5-hydroxy indan-(1E)-ylidene)acetic acid.

frequency doubling. With the second beam, a white light continuum was generated by focusing it on a 2-mm quartz plate. The excitation pulse from the BBO crystal was focused in the sample to a diameter of ~130 μm and spatially overlapped with the smaller probe beam. The overlap between pump beam and probe beam was carefully checked to be homogeneous by means of spectral shape comparison on variation of the pump spot size. The absorption changes in the visible were recorded after dispersion in a spectrograph, with a 256-element diode array (S4801-256Q; Hamamatsu, Hamamatsu City, Japan). The pump beam was polarized at the magic-angle orientation (54.7°) with respect to the probe beam using a Berek polarizer. The sample was moved during the measurement in a Lissajous scanner to ensure a fresh spot for every excitation pulse. A phase-locked chopper operating at 500 Hz was used to ensure that on every other shot the sample was excited and the changes in transmission, and hence optical density, could be measured. The time delay between the pump and probe beam was controlled by sending the pump beam over a moveable delay line. The instrument response function, determined via the cross correlation of pump and probe, was ~150 fs. For each experiment, ~100 time-gated spectra were recorded between −10 ps and 2.5 ns relative to the maximum of the instrument response function. All experiments were performed at room temperature.

Set-up for μs/ms time-resolved visible spectroscopy

An Edinburgh Instruments LP900 spectrometer (Livingston, West Lothian, United Kingdom) equipped with a photomultiplier, in combination with a Continuum Surelite OPO laser (for further details, see Hendriks et al. (34)) was used for μs/ms time-resolved visible spectroscopy. PYP samples were excited with 446-nm laser flashes of ~5–6 mJ/pulse (pulse duration 6 ns). Time traces were recorded for the four proteins at 360 nm, ~446 nm, and between 484 and 503 nm (dependent on the λ^{max} of the particular protein), with the slow-board option of the photomultiplier (time resolution ~2 μs). Optical interference filters were used before the sample to minimize measurement artifacts induced by probe light.

Transient ms/s UV-vis spectroscopy

UV-vis spectra were recorded using an HP8453 UV-vis spectrophotometer (Hewlett Packard, Palo Alto, CA). Time-resolved spectra were recorded from 250 to 600 nm, using an integration time of 0.1 s. A Kraayenhof cuvette was used to thermostat the sample at 25°C, with simultaneous pH recording. A Schott KL1500 LCD lamp was used to illuminate the samples with wild-type or R52A protein. For the rotation-locked proteins, a microsecond flash lamp was used.

Steady-state fluorescence

Steady-state fluorescence spectra were recorded on a Fluorolog 3 spectrometer (Spex, Metuchen, NJ) with a 450-W Xe lamp as the excitation light source. The excitation wavelength was set at the absorption maximum of the respective protein (see Fig. 2 below), and emission was recorded from 450 to 600 nm for the two rotation-locked derivatives (i.e., the wild-type (WTRL) and R52ARL) and from 455 to 600 nm (with a slit width of 5 nm) for the two proteins reconstituted with *p*-coumaric acid (i.e., wild-type and R52A). The slit width for the excitation and emission light was set at 0.5 and 5 μm, respectively, for all four samples.

Synthesis of (5-hydroxy indan-(1E)-ylidene)acetic acid (rotation-locked chromophore)

After protection of its phenolic hydroxy group with *tert*-butyl-dimethyl-silanyloxyl chloride, ~300 mg of (5-hydroxy-indan-(1E)-ylidene)-acetic acid (190.20 mol wt) was synthesized from 5-hydroxy-1-indanone through coupling with diethylphosphonoacetate. The phenolic hydroxyl group was deprotected with tetra-*n*-butyl-ammonium fluoride. For this synthesis, reagents were purchased at the highest commercial quality available and used without further purification. Flash chromatography was carried out with ACROS silica gel (particle size 35–70 μm). Infrared spectra were recorded using an IFS 28 spectrophotometer (Bruker, Billerica, MA), NMR spectra were obtained using a Bruker ARX 400 spectrometer (400 MHz), and accurate mass values of intermediates and the final product were recorded on a JMS SX/SX102A four-sector mass spectrometer (JEOL, Tokyo, Japan), coupled to a JEOL MS-MP7000 data system or a TSQ7000 mass spectrometer (Thermo Finnigan, San Jose, CA) using Xcaliber 1.2 software for acquisition and data processing.

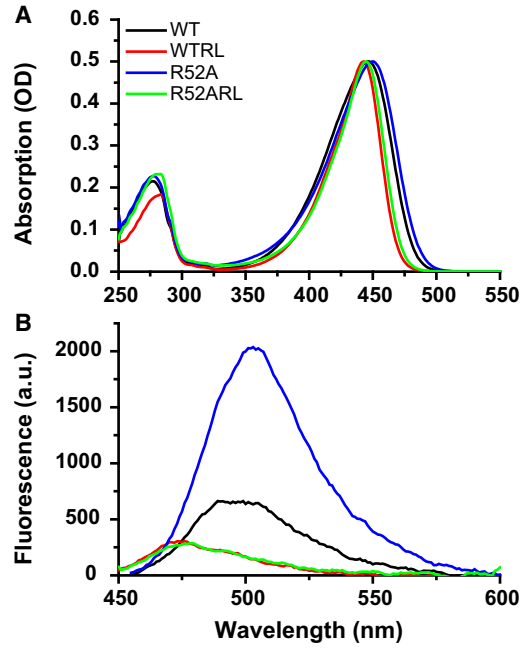

FIGURE 2 Characterization of the static UV-vis absorbance and fluorescence emission of the four PYP derivatives. (*A*) Absorption spectra of wild-type PYP (*black*), WTRL (*red*), R52A (*blue*), and R52ARL (*green*) in 20 mM Tris buffer, pH 8.0. The absorption maxima are centered at 446, 443, 450, and 445 nm, respectively. (*B*) The corresponding emission spectra, with excitation of all samples at their respective absorbance maxima.

Site-directed mutagenesis

Site-directed mutagenesis was performed using the QuikChange kit (Stratagene, La Jolla, CA) and confirmed by DNA sequencing, as described previously (35).

Sample preparation

Wild-type PYP and its R52A mutant derivative were produced and isolated as described previously for wild-type PYP (36). Apo-PYP was reconstituted with the 1,1′-carbonyldiimidazole derivative of *p*-coumaric acid or rotation-locked chromophore, as described by Hendriks et al. (37). The reconstituted holoproteins were purified in two subsequent steps, with Ni-affinity and anion-exchange chromatography, respectively (37). The purified holoproteins were used without removing the genetically introduced N-terminal hexahistidine-containing tag, in a buffer containing 20 mM Tris-HCl,

pH 8.0. The purity index for all samples was >0.5, except for R52A PYP reconstituted with *p*-coumaric acid, in which case it was >0.75.

For measurements at pH 5, 8, and 10, buffer solutions containing 20 mM acetic acid, 20 mM Na2HPO4, 20 mM Tris, and 20 mM boric acid, with the same ionic strength, were prepared as described previously (17). For ultrafast spectroscopy, samples were concentrated to a final optical density of ~0.3 at 400 nm in a 50-μm-thick cell constructed from two CaF2 windows separated by a Teflon spacer.

Data analysis

The transient difference absorption spectra were subjected to global and target analysis, as reviewed in van Stokkum et al. (38). Briefly, the basis of global analysis is the superposition principle, which states that the measured $\psi(t,\lambda)$ data result from a superposition of the spectral properties, $\varepsilon_l(\lambda)$, of the components present in the system of interest weighted by their concentration $c_l(t)$.

$$\psi(t,\lambda) = \sum_{l=1}^{n_{comp}} c_l(t)\varepsilon_l(\lambda)$$

The $c_l(t)$ of all n_{comp} components are described by a compartmental model that consists of first-order differential equations, with sums of exponential decays as solution. We will consider two types of compartmental model: 1), a sequential model with increasing lifetimes, also called an unbranched unidirectional model, which results in evolution-associated difference spectra (EADS); and 2), a full compartmental scheme, possibly including branchings and equilibria, which yields species-associated difference spectra (SADS). The latter is most often referred to as target analysis, where the target is the proposed kinetic scheme, including specific spectral assumptions.

With ultrafast spectroscopy, the instrument response function can usually adequately be modeled with a Gaussian with parameters for location and full width at half-maximum (typically 100–250 fs). The dispersion of this location parameter is described by a polynomial. All exponential decays from the above models have to be convolved with this instrument response function.

RESULTS

After heterologous overexpression in *Escherichia coli* and purification, the four proteins studied in this investigation, i.e., wild-type and R52A-PYP reconstituted with 4-hydroxy-cinnamic acid and (5-hydroxy indan-(1E)-yli dene)acetic acid, respectively (see Fig. 1 for an overview of the structure of their chromophore-binding pocket), were characterized with static UV-vis spectroscopy (Fig. 2 *A*). The results show that whereas the R52A mutation causes a slight red shift (4 nm for samples containing the *p*-coumaryl chromophore), the two rotation-lock PYPs show a modest blue shift. The full width at half-maximum of the latter spectra, however, is significantly smaller than that of the two samples reconstituted with the endogenous chromophore, *p*-coumaric acid, presumably due to a much smaller contribution of the vibronic sideband of the main electronic transition of PYP. The decrease in the dynamic Stokes shift in the fluorescence emission spectra of the two rotation-locked PYPs is even more pronounced, shifting from >500 nm for the endogenous chromophore to <475 nm (Fig. 2 *B*) for the rotation-locked derivatives. This figure also reveals that the already low fluorescence quantum yield of PYP is even lower (~50%) in the rotation-locked derivatives, whereas substitution of R52 by an alanine results in an almost threefold increase of this yield.

Next, time-resolved visible pump/visible probe measurements in the 100 fs to 2 ns time domain were performed on all four samples, using 400-nm excitation. All four samples show rich dynamics in which some trends are immediately apparent, like the more extensive ultrafast relaxation in the rotation-lock PYPs leading to a significantly shorter-lived signal than in wild-type PYP (see Fig. S1 in the Supporting Material for a set of transients of all four samples collected at 446 nm, derived from the time-gated spectra). However, much more detail is visible in the analysis of the corresponding EADS (Fig. S2). An optimal fit to the data requires four lifetimes for each sample plus a component that does not decay on the timescale of our experiment (i.e., >>2.7 ns).

These EADS clearly show that the two rotation-locked proteins have 1), a smaller red-shifted stimulated emission with respect to the 510-nm position at which the stimulated-emission band of the coumaryl derivatives is centered, consistent with their fluorescence characteristics (Fig. 2 *B*); 2), significantly faster and monoexponential excited-state decay (decay in 0.5 and 0.6 ps, respectively, versus the 0.7–7 ps in wild-type), as can be concluded from the disappearance of the contribution of stimulated emission from the subsequent spectra in each series of EADS; 3), both rotation-locked proteins form decreased amounts of the primary photoproducts (the blue and green spectra can be assigned to the states I_0 and I_1, with product absorption bands at ~485 and 475 nm, respectively). Note that the product bands of the rotation-locked proteins appear to be slightly blue-shifted, which may result in partial cancellation of their absorbance with the bleached ground-state absorption, thus making a reliable estimate of the amount of these products formed difficult; and finally, 4), the rotation-locked proteins display an intermediate spectrum with a 3-ps lifetime that resembles the spectrum of the GSI of wild-type PYP resolved in pump-dump-probe experiments (18,39) and target analysis (A. Rupenyan and M. L. Groot, unpublished).

However, to be able to characterize in more detail these initial photocycle steps and the distinct spectral characteristics of the various intermediates formed upon photoactivation in these four proteins, a target analysis of the data is required. A complication in this analysis is the multiplicity of the excited state of each sample: the decay of the excited state has to be fitted by up to three time constants, and in a similar way, the appearance of I_0 can be described with two to three time constants. From these excited states, the yield of I_0 formation is largest for the shorter-lived excited states, in agreement with previous observations (see, e.g., works by Larsen and colleagues (18,32)). However, the target analysis of the spectral data of the two rotation-locked proteins already provides satisfactory results using a single

excited state. Therefore, to facilitate comparison between the four samples here, we have fitted the datasets obtained with the two proteins reconstituted with the *p*-coumaryl chromophore (i.e., wild-type PYP and R52A) with a single component for the excited-state decay as well, at the cost of a small decrease in root-mean-squared value.

The results of this target analysis (see Fig. 3) and the corresponding table with rate constants (see Table S1) provide more quantitative information on the systems dynamics in the four proteins and give information beyond that derived from the global analysis (e.g., the quantum yields). From this target analysis, it is clear that rotation-locking of the chromophore causes not only much faster excited-state decay but also an almost twofold lower quantum yield of photochemistry. We were surprised to find that in the latter two samples this is accompanied by the absence of internal conversion directly to the ground state, presumably because the free-energy barrier for the transition that leads to the GSI is even lower. The result is that in these two samples, the quantum yield of formation of the GSI state reaches values that approach unity (i.e., 83%). The spectral characteristics of these intermediates are consistent with the above observations (Fig. 4): the stimulated emission of the rotation-locked proteins is blue-shifted to the extent that it is only visible as a broadening of the low-energy shoulder of the ground-state bleach. The corresponding I_0 and GSI have not only a blue-shifted absorption maximum (~25 nm for I_0), but also a smaller molar extinction coefficient. For the GSI, it is difficult to estimate the λ_{max} because of the extensive overlap with ground-state depletion. The I_1 intermediates show the expected blue shift relative to their corresponding I_0 states, except in the case of the I_1 state of the R52A protein, which is almost isoenergetic with its I_0.

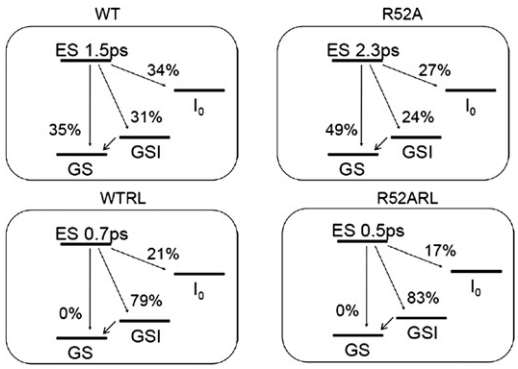

FIGURE 3 Target-model-based analysis of the initial stages of the photocycle of the four PYP derivatives. I_0 decays into I_1 with a time constant of ~1 ns and a yield of 100%. The fitted lifetimes and relative populations of the states accessible from the ES are shown. The excited states of wild-type and R52A were found to decay biexponentially with time constants of 0.7 and 6.8 ps and 1.9 and 27 ps, respectively, with the quantum yield of I_0 formation largest for the fastest fraction, in agreement with Larsen et al. (18). To facilitate comparison with the rotation-locked samples, the data for excited-state decay for all four proteins were fitted here with single exponents of 1.5 ps and 2.3 ps, respectively. The yield of the ground state in WTRL and R52ARL is very low, and can be fitted with yields between 0 and 10%. The reduction of this yield and that of I_0 in the rotation-locked samples is due to a four- to sixfold increase in the rate of ES → GSI.

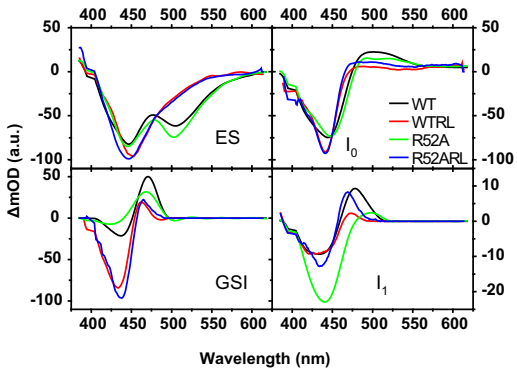

FIGURE 4 Species-associated difference spectra (SADS) of the four PYP derivatives, obtained from fitting the target model of Fig. 3 to the data. The SADS of wild-type PYP are in good agreement with earlier reports in the literature (e.g., (18,39). The GSI spectrum of the rotation-locked samples is easily resolved, as it appeared pronounced in the data, as shown in Fig. S2. The quantum yields depicted in Fig. 3 were determined by scaling the SADS of each state to that of the ES, which may result in ~10% uncertainty. An exception is the I_1 state, for which we have used a yield of 100% for the I_0 to I_1 transition, as determined with femtosecond midinfrared spectroscopy (14,19). Color code as in Fig. 2.

The results obtained to date have revealed that within this set of four proteins, R52A is the most similar to wild-type PYP. One would expect the rotation-locked samples to be more similar to wild-type PYP, but different from R52A PYP if the charge on R52 were steering the primary photochemistry of PYP toward single-bond rotation (see above). As this observation is clearly different from what has been predicted by theory (17,30), we tested a second approach in which the charge on R52 is varied.

By varying the pH of the buffer in the range 5–10, we modulated the net charge of the side chain of R52 (see Discussion) and, by consequence, the environmental electrostatics of the *p*-coumaryl chromophore. The results presented in Fig. 5 reveal that the primary photochemistry in PYP is totally invariant with pH in this pH range. This applies to both the observed lifetimes and the shape of the difference spectra.

Locking the rotation around the C4-C7 bond not only has consequences for the ultrafast photochemistry of PYP but might also affect the slower processes that occur in the photocycle of PYP. We therefore also analyzed the μs/ms time-resolved visible absorption changes at three different wavelengths: 360 nm, at which the main contribution is from pB intermediates; in the range 484–503 nm, to record the contribution of the red-shifted intermediates (i.e., pR) (see also Table S2); and $\approx$446 nm, the absorbance maximum of the four proteins, at which bleaching of pG and absorption of pR contribute to the dynamics of the changes in UV-vis absorbance. The absorbance traces at 360 nm are of particular interest, because at this wavelength

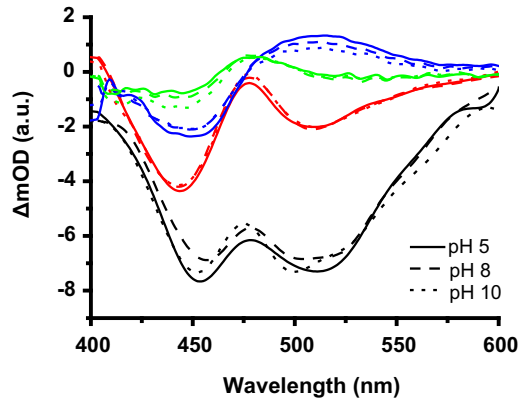

FIGURE 5 pH dependence of the ultrafast kinetics of wild-type PYP. At each pH, the dynamics could be fitted with four time constants. The EADS for each time constant are indicated: 0.9, 0.9, and 0.8 ps (*black*); 6, 5, and 5.5 ps (*red*); 1.4, 1.7, and 1.4 ns (*blue*), and infinite (*green*), for wild-type PYP at pH 5, 8, and 10, respectively.

both the decay of the I_1/pR state (which coincides with formation of pB′ (20)) and the thermal recovery of the ground state can be observed. The results obtained (Fig. 6) clearly reveal that the R52A mutation accelerates pB′ formation (in combination with the *p*-coumaryl chromophore) and retards ground-state recovery. This is similar to the effect observed by others (e.g., Hellingwerf et al. (4) and Cusanovich and Meyer (5)) in R52Q and several other mutant proteins. A global analysis of these data (Table S2, Fig. S3, and Fig. S4) furthermore shows that the effect of replacing the *p*-coumaryl chromophore with the rotation-locked chromophore is an approximately five- and ninefold retardation of the rate of formation of the first blue-shifted state for wild-type PYP and R52A, respectively, whereas the recovery reaction (i.e., the re-formation of pG) for these proteins is accelerated 8- and 16-fold, respectively. However, the data for the two rotation-locked proteins in this time domain are well-fitted with a sum of two exponentials

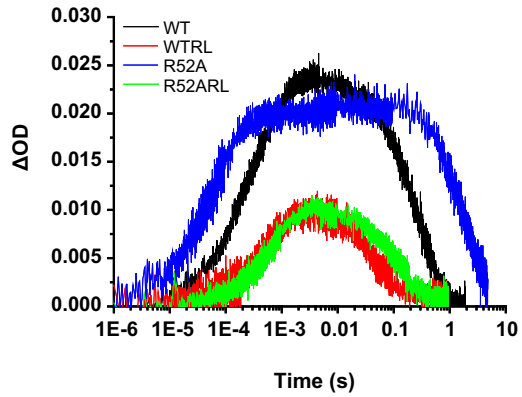

FIGURE 6 Time traces of the absorbance changes during the later part of the photocycle of the four PYP derivatives, recorded at 360 nm. The pB intermediates absorb maximally at 360 nm. Their rise and decay can be fitted with the time constants, as shown in Table S2 (see Fig. S1). Color code as in Fig. 2.

(Table S2), whereas for the wild-type protein, at least three exponentials are required (26). We therefore carried out a target analysis of this same data set based on the photocycle scheme pR ↔ pB′ → pB → pG. For the wild-type protein, the results obtained confirm previous observations (5,24,26), whereas the data obtained with the R52A protein show that this mutation particularly accelerates proton transfer from E46 to the chromophore (i.e., pR → pB′) and also decelerates pG recovery (Table 1). We therefore tentatively conclude that single-bond rotation around the C4-C7 bond contributes to both of these processes. The slower part of the photocycle of the two rotation-locked proteins is well described by the sequential model pR → pB → pG, in which a single exponent suffices to describe the pR to pB transition. The estimated SADS (see Fig. S5) are consistent with the expected shapes for pR and pB, establishing the suitability of these two photocycle schemes for the two sets of proteins (i.e., wild-type and R52A on the one hand and WTRL and R52ARL on the other.

DISCUSSION

In the past, the use of various rotation-locked chromophores has provided important information on the primary photochemistry in the two largest and most diverse families of photosensory receptors that use E/Z/E isomerization of their chromophore to initiate the biological signaling process, i.e., the rhodopsins (40,41) and the phytochromes (42). For the xanthopsin family also, chromophore derivatives with the C_7=C_8 ethylenic bond of the chromophore locked in the *trans* and *cis* states, respectively, have been exploited to better understand the molecular basis of functioning of this family (43,44).

Here, we have made use of yet another rotation-locked chromophore, i.e., one in which rotation of the C_4-C_7 single bond is prevented by making it part of a cyclopentane ring. This restricts the flexibility within this chromophore even more than it does within derivatives in which a cyclohexane ring is used instead (45). This rotation-locked analog has been used to reconstitute wild-type PYP and a mutant

TABLE 1 Target analysis of the transitions between the intermediates of the photocycle of PYP in the microsecond-to-second time domain

PYP derivative	pR → pB′	pB′ → pR	Δ*G* (meV)*	pB′ → pB	pB → pG
Wild-type	3.65	1.72	19	2.02	0.00366
R52A	15.2	0.97	71	2.71	0.00049
		pR → pB			
WTRL		1.37			0.0276
R52ARL		1.76			0.0076

Estimated rate constants (ms^{-1}) of the transitions between intermediates. Kinetic scheme for wild-type and R52A: pR ↔ pB′ → pB → pG.
*Δ*G* of the reaction between pR and pB′. Kinetic scheme for WTRL and R52ARL: pR → pB → pG.

with an altered amino acid at position 52, R52A. Although studies were available in the literature on the nanosecond-to-microsecond spectroscopic characterization of the R52Q mutant of PYP, here we have used the R52A mutant to have the arginine substituted by the even less polar amino acid alanine, and we have characterized this protein at higher time resolution. Nevertheless, with respect to the quantum yield, absorbance maxima, and dynamics characteristics, the two mutants are quite similar (31,46,47).

The results of the ultrafast spectroscopy have been shown to be very similar between the two rotation-locked samples on the one hand and the two PYP derivatives reconstituted with *p*-coumaryl chromophore on the other. If the charged R52 had been decisive for the occurrence of C=C double-bond isomerization (17), one would have predicted a much larger difference between the wild-type and R52A PYP isomerization. It seems to us that in this aspect, the computational description of Z/E isomerization in PYP has to be refined. Conversely, the two rotation-locked proteins are similar in their spectroscopic properties and their dynamics, and show a reduced, but not blocked, product formation. Therefore, we conclude that the flexibility to rotate around the C_4-C_7 bond is necessary for maximal yields of photochemistry in PYP. We think that it will be revealing in future computational analyses of PYP to include studies of protein reconstituted with this single-bond rotation-locked chromophore, to provide a firm theoretical basis for our observations. It is relevant to note that considering the mechanism of isomerization of the C_7=C_8 ethylenic bond in PYP, which is followed by a rotary movement of the carbonyl group around the long axis of the *p*-coumaryl chromophore, single-bond rotation around the C-S bond and/or around single bonds within C69 may also be part of the primary photochemistry in PYP. Several additional features reported in this study form a challenge for future calculations based on first principles. A relevant example is the relatively blue peak position of the rotation-locked derivatives in the I_0 state (Fig. 4).

For the rotation-locked proteins, just a single excited-state (ES) compartment was sufficient to fit the ultrafast transient absorption data. This suggests that the multiphasic nature of the decay of the ES, which for wild-type PYP needs to be fitted with up to three ES compartments (18) (A. Rupenyan and M. L. Groot, unpublished results), is an inherent property of the chromophore and is absent in the rotation-locked samples. Furthermore, the increased rigidity of the locked chromophore abolishes internal conversion (Fig. 3), which is according to expectation based on theory set forth by others (e.g., Seidner and Domcke (48) and Abbruzzetti et al. (49)), and approximately halves the quantum yields of photochemistry and fluorescence in the two rotation-locked proteins. As a result, the contribution of decay of the ES through the channel for GSI formation has increased, up to 0.83 in rotation-locked R52A PYP. This latter observation will aid in the further characterization of the precise configuration of this GSI intermediate with time-resolved infrared spectroscopy (14,19).

Although biochemistry textbooks generally quote a value of ~12.5 for the pK of the side chain of an arginine (see, e.g, Berg et al. (50)), the value for R52 in PYP must be much lower. First, in the neutron diffraction study of PYP that revealed the existence of the low-barrier hydrogen bond between E46 and the chromophore, it was observed that even at pH 7.5 (the pH of the mother liquor), R52 was fully uncharged (11). This result implies that the pK of R52 is $<$7.5, although this pK might be tuned slightly because R52 is a surface residue. In this respect, it is relevant to note that a recent study in which an NMR titration of all amino acids of PYP was presented revealed that R52 has a pK of 8.7 (F. A. A. Mulder, unpublished). Hence, one can safely assume that the net charge of R52 will change from positive to neutral when one increases the pH from 5 to 10. As in this transition the primary photochemistry of PYP remains unaltered (Fig. 5), this provides independent evidence that the charge on R52 does not have a profound effect on the outcome of the isomerization process in the chromophore of PYP that follows (blue) light absorption.

Restriction of the rotation across the C4-C7 bond also significantly affects the kinetics in the intermediate and slower parts of the photocycle of PYP. Two effects are distinguishable: the rate of formation of the blue-shifted intermediate is decreased, and its rate of decay is accelerated (Table 1). Both effects are compatible with the interpretation that the pB state of the rotation-locked proteins represents an incompletely unfolded signaling state, leading to the prediction that its absorbance maximum is slightly red-shifted compared to the corresponding intermediate of wild-type PYP (26,51). Apparently, hindering C4-C7 single-bond rotation increases the time it takes to bring E46 and the chromophore into a position that allows unidirectional proton transfer, which in turn leads to a less stable signaling state.

Comparing wild-type PYP with R52A shows that this mutation stabilizes the pB state with respect to pR (Table 1, *column 4*). Considering the recovery rates of the two proteins, it may well be that this is due to stabilization of pB in the R52A protein, but a strained chromophore may of course also destabilize pR. It has been reported that R52 in the pB state hydrogen-bonds to the chromophore (52). However, as this observation was made on a pB state confined in a crystal lattice, whereas the pB states in solution appear to be quite different (53,54), we do not think that such direct hydrogen-bonding is involved.

The effects of the restricted single-bond rotation, and the R52A mutation, on the photocycle kinetics turn out to be additive, so that in the R52ARL protein, the recovery rate is close to that of wild-type PYP.

A comparison of the maximal increase in absorbance at 360 nm and the maximal decrease at 446 nm (Fig. 6 and

Fig. S5) using the microsecond/millisecond data from wild-type PYP as a reference also allows an independent estimate of the quantum yield of these PYP derivatives. Considering the accuracy with which such data can be measured, the data obtained are consistent with the results displayed in Fig. 3: An approximately twofold decrease is caused by the rotation-locked chromophore.

It will be of interest to test this and other chromophore analogs on the phototactic capabilities of *H. halophila*, similar to the way they were exploited in *Idiomarina halophila* (44).

CONCLUSIONS

We have studied the isomerization pathway of PYP and the role of the charge of the side chain of amino acid R52 therein by selectively locking one of the single bonds of the chromophore. Preventing rotation of the C4-C7 chromophore bond enhances the rate of formation of a nonproductive intermediate state, GSI, and leads to reduction of the physiological Z/E isomerization of the chromophore. These results confirm that C4-C7 single-bond rotation in PYP is not an alternative to C7=C8 double-bond rotation but appears to optimize double-bond isomerization (e.g., with a compensatory movement). The initial photocycle dynamics of PYP were observed to be not significantly affected by the charge of the amino acid residue at position 52, which was varied by 1), varying the pH of the sample between 5 and 10; and 2), site-directed mutagenesis to construct R52A**.**

SUPPORTING MATERIAL

Two tables and five figures are available at http://www.biophysj.org/biophysj/supplemental/S0006-3495(11)00836-8.

The authors thank Dr. Jan van Maarseveen (Van 't Hoff Institute of Molecular Sciences, University of Amsterdam) for synthesis of (5-hydroxy indan-(1E)-ylidene)acetic acid and Mr. Jos Thieme and Mr. Jos Arents for excellent technical support.

K.J.H. and R.v.G. acknowledge support from the Human Frontier Science Program through grant number HFSP-RGP0038/2006.

REFERENCES

1. van der Horst, M. A., and K. J. Hellingwerf. 2004. Photoreceptor proteins, "star actors of modern times": a review of the functional dynamics in the structure of representative members of six different photoreceptor families. *Acc. Chem. Res.* 37:13–20.
2. Meyer, T. E. 1985. Isolation and characterization of soluble cytochromes, ferredoxins and other chromophoric proteins from the halophilic phototrophic bacterium *Ectothiorhodospira halophila*. *Biochim. Biophys. Acta.* 806:175–183.
3. Sprenger, W. W., W. D. Hoff, …, K. J. Hellingwerf. 1993. The eubacterium *Ectothiorhodospira halophila* is negatively phototactic, with a wavelength dependence that fits the absorption spectrum of the photoactive yellow protein. *J. Bacteriol.* 175:3096–3104.
4. Hellingwerf, K. J., J. Hendriks, and T. Gensch. 2003. Photoactive yellow protein, a new type of photoreceptor protein: will this "yellow lab" bring us where we want to go? *J. Phys. Chem. A.* 107:1082–1094.
5. Cusanovich, M. A., and T. E. Meyer. 2003. Photoactive yellow protein: a prototypic PAS domain sensory protein and development of a common signaling mechanism. *Biochemistry.* 42:4759–4770.
6. Imamoto, Y., and M. Kataoka. 2007. Structure and photoreaction of photoactive yellow protein, a structural prototype of the PAS domain superfamily. *Photochem. Photobiol.* 83:40–49.
7. Van Beeumen, J. J., B. V. Devreese, …, M. A. Cusanovich. 1993. Primary structure of a photoactive yellow protein from the phototrophic bacterium *Ectothiorhodospira halophila*, with evidence for the mass and the binding site of the chromophore. *Protein Sci.* 2:1114–1125.
8. Kim, M., R. A. Mathies, …, K. J. Hellingwerf. 1995. Resonance Raman evidence that the thioester-linked 4-hydroxycinnamyl chromophore of photoactive yellow protein is deprotonated. *Biochemistry.* 34:12669–12672.
9. Borgstahl, G. E. O., D. R. Williams, and E. D. Getzoff. 1995. 1.4 Å structure of photoactive yellow protein, a cytosolic photoreceptor: unusual fold, active site, and chromophore. *Biochemistry.* 34:6278–6287.
10. Kort, R., H. Vonk, …, K. J. Hellingwerf. 1996. Evidence for *trans-cis* isomerization of the *p*-coumaric acid chromophore as the photochemical basis of the photocycle of photoactive yellow protein. *FEBS Lett.* 382:73–78.
11. Yamaguchi, S., H. Kamikubo, …, M. Kataoka. 2009. Low-barrier hydrogen bond in photoactive yellow protein. *Proc. Natl. Acad. Sci. USA.* 106:440–444.
12. Gensch, T., C. C. Gradinaru, …, R. van Grondelle. 2002. The primary photoreaction of photoactive yellow protein (PYP): anisotropy changes and excitation wavelength dependence. *Chem. Phys. Lett.* 356:347–354.
13. van Brederode, M. E., T. Gensch, …, S. E. Braslavsky. 1995. Photoinduced volume change and energy storage associated with the early transformations of the photoactive yellow protein from *Ectothiorhodospira halophila*. *Biophys. J.* 68:1101–1109.
14. Groot, M. L., L. J. van Wilderen, …, R. van Grondelle. 2003. Initial steps of signal generation in photoactive yellow protein revealed with femtosecond mid-infrared spectroscopy. *Biochemistry.* 42:10054–10059.
15. Xie, A., W. D. Hoff, …, K. J. Hellingwerf. 1996. Glu^{46} donates a proton to the 4-hydroxycinnamate anion chromophore during the photocycle of photoactive yellow protein. *Biochemistry.* 35:14671–14678.
16. Groenhof, G., M. F. Lensink, …, A. E. Mark. 2002. Signal transduction in the photoactive yellow protein. I. Photon absorption and the isomerization of the chromophore. *Proteins.* 48:202–211.
17. Groenhof, G., L. V. Schäfer, …, M. A. Robb. 2008. Arginine52 controls the photoisomerization process in photoactive yellow protein. *J. Am. Chem. Soc.* 130:3250–3251.
18. Larsen, D. S., I. H. van Stokkum, …, R. van Grondelle. 2004. Incoherent manipulation of the photoactive yellow protein photocycle with dispersed pump-dump-probe spectroscopy. *Biophys. J.* 87:1858–1872.
19. van Wilderen, L. J., M. A. van der Horst, …, M. L. Groot. 2006. Ultrafast infrared spectroscopy reveals a key step for successful entry into the photocycle for photoactive yellow protein. *Proc. Natl. Acad. Sci. USA.* 103:15050–15055.
20. Xie, A., L. Kelemen, …, W. D. Hoff. 2001. Formation of a new buried charge drives a large-amplitude protein quake in photoreceptor activation. *Biochemistry.* 40:1510–1517.
21. Van Brederode, M. E., W. D. Hoff, …, K. J. Hellingwerf. 1996. Protein folding thermodynamics applied to the photocycle of the photoactive yellow protein. *Biophys. J.* 71:365–380.
22. Meyer, T. E., E. Yakali, …, G. Tollin. 1987. Properties of a water-soluble, yellow protein isolated from a halophilic phototrophic bacterium that has photochemical activity analogous to sensory rhodopsin. *Biochemistry.* 26:418–423.

23. Hoff, W. D., I. H. van Stokkum, …, K. J. Hellingwerf. 1994. Measurement and global analysis of the absorbance changes in the photocycle of the photoactive yellow protein from *Ectothiorhodospira halophila*. *Biophys. J.* 67:1691–1705.
24. Hendriks, J., I. H. M. van Stokkum, and K. J. Hellingwerf. 2003. Deuterium isotope effects in the photocycle transitions of the photoactive yellow protein. *Biophys. J.* 84:1180–1191.
25. Hoersch, D., H. Otto, …, M. P. Heyn. 2007. Role of a conserved salt bridge between the PAS core and the N-terminal domain in the activation of the photoreceptor photoactive yellow protein. *Biophys. J.* 93:1687–1699.
26. Hendriks, J., and K. J. Hellingwerf. 2009. pH Dependence of the photoactive yellow protein photocycle recovery reaction reveals a new late photocycle intermediate with a deprotonated chromophore. *J. Biol. Chem.* 284:5277–5288.
27. Premvardhan, L. L., M. A. van der Horst, …, R. van Grondelle. 2003. Stark spectroscopy on photoactive yellow protein, E46Q, and a nonisomerizing derivative, probes photo-induced charge motion. *Biophys. J.* 84:3226–3239.
28. Grabowski, Z. R., K. Rotkiewicz, …, W. Baumann. 1979. Twisted intra-molecular charge-transfer states (TICT)—new class of excited-states with a full charge separation. *Nouv. J. .Chim.* 3:443–454.
29. Grabowski, Z. R., K. Rotkiewicz, and W. Rettig. 2003. Structural changes accompanying intramolecular electron transfer: focus on twisted intramolecular charge-transfer states and structures. *Chem. Rev.* 103:3899–4032.
30. Ko, C., A. M. Virshup, and T. J. Martinez. 2008. Electrostatic control of photoisomerization in the photoactive yellow protein chromophore: ab initio multiple spawning dynamics. *Chem. Phys. Lett.* 460:272–277.
31. Changenet-Barret, P., P. Plaza, …, M. Kataoka. 2007. Role of arginine 52 on the primary photoinduced events in the PYP photocycle. *Chem. Phys. Lett.* 434:320–325.
32. Larsen, D. S., and R. van Grondelle. 2005. Initial photoinduced dynamics of the photoactive yellow protein. *ChemPhysChem.* 6:828–837.
33. Groot, M. L., L. J. G. W. van Wilderen, and M. Di Donato. 2007. Time-resolved methods in biophysics. 5. Femtosecond time-resolved and dispersed infrared spectroscopy on proteins. *Photochem. Photobiol. Sci.* 6:501–507.
34. Hendriks, J., W. D. Hoff, …, K. J. Hellingwerf. 1999. Protonation/deprotonation reactions triggered by photoactivation of photoactive yellow protein from *Ectothiorhodospira halophila*. *J. Biol. Chem.* 274:17655–17660.
35. van Aalten, D. M. F., A. Haker, …, W. Crielaard. 2002. Engineering photocycle dynamics. Crystal structures and kinetics of three photoactive yellow protein hinge-bending mutants. *J. Biol. Chem.* 277:6463–6468.
36. Kort, R., W. D. Hoff, …, K. J. Hellingwerf. 1996. The xanthopsins: a new family of eubacterial blue-light photoreceptors. *EMBO J.* 15:3209–3218.
37. Hendriks, J., T. Gensch, …, J. J. van Thor. 2002. Transient exposure of hydrophobic surface in the photoactive yellow protein monitored with Nile Red. *Biophys. J.* 82:1632–1643.
38. van Stokkum, I. H. M., D. S. Larsen, and R. van Grondelle. 2004. Global and target analysis of time-resolved spectra. *Biochim. Biophys. Acta.* 1657:82–104.
39. Changenet-Barret, P., P. Plaza, …, M. Kataoka. 2009. Structural effects on the ultrafast photoisomerization of photoactive yellow protein. Transient absorption spectroscopy of two point mutants. *J. Phys. Chem. C.* 113:11605–11613.
40. Birge, R. R., L. P. Murray, …, K. Nakanishi. 1985. Two-photon spectroscopy of locked-11-*cis*-rhodopsin: evidence for a protonated Schiff base in a neutral protein binding site. *Proc. Natl. Acad. Sci. USA.* 82:4117–4121.
41. Akita, H.…, 1980. Non-bleachable rhodopsins retaining the full natural chromophore. *J. Am. Chem. Soc.* 102:6370–6372.
42. Inomata, K., M. A. Hammam, …, T. Lamparter. 2005. Sterically locked synthetic bilin derivatives and phytochrome Agp1 from Agrobacterium tumefaciens form photoinsensitive Pr- and Pfr-like adducts. *J. Biol. Chem.* 280:24491–24497.
43. Cordfunke, R., R. Kort, …, K. J. Hellingwerf. 1998. *Trans*/*cis* (Z/E) photoisomerization of the chromophore of photoactive yellow protein is not a prerequisite for the initiation of the photocycle of this photoreceptor protein. *Proc. Natl. Acad. Sci. USA.* 95:7396–7401.
44. van der Horst, M. A., T. P. Stalcup, …, W. D. Hoff. 2009. Locked chromophore analogs reveal that photoactive yellow protein regulates biofilm formation in the deep sea bacterium *Idiomarina loihiensis*. *J. Am. Chem. Soc.* 131:17443–17451.
45. Sheves, M., N. Friedman, …, M. Ottolenghi. 1985. Primary photochemical event in bacteriorhodopsin: study with artificial pigments. *Biochemistry.* 24:1260–1265.
46. Borucki, B., J. A. Kyndt, …, M. P. Heyn. 2005. Effect of salt and pH on the activation of photoactive yellow protein and gateway mutants Y98Q and Y98F. *Biochemistry.* 44:13650–13663.
47. Philip, A. F., R. A. Nome, …, W. D. Hoff. 2010. Spectral tuning in photoactive yellow protein by modulation of the shape of the excited state energy surface. *Proc. Natl. Acad. Sci. USA.* 107:5821–5826.
48. Seidner, L., and W. Domcke. 1994. Microscopic modelling of photoisomerization and internal-conversion dynamics. *Chem. Phys.* 186:27–40.
49. Abbruzzetti, S., R. Bizzarri, …, F. Beltram. 2010. Photoswitching of E222Q GFP mutants: "concerted" mechanism of chromophore isomerization and protonation. *Photochem. Photobiol. Sci.* 9:1307–1319.
50. Berg, J. M., J. L. Tymoczko, and L. Stryer. 2012. Biochemistry, 7th ed. W. H. Freeman, New York.
51. Yeremenko, S., I. H. van Stokkum, …, K. J. Hellingwerf. 2006. Influence of the crystalline state on photoinduced dynamics of photoactive yellow protein studied by ultraviolet-visible transient absorption spectroscopy. *Biophys. J.* 90:4224–4235.
52. Genick, U. K., G. E. Borgstahl, …, E. D. Getzoff. 1997. Structure of a protein photocycle intermediate by millisecond time-resolved crystallography. *Science.* 275:1471–1475.
53. Vreede, J., W. Crielaard, …, P. G. Bolhuis. 2005. Predicting the signaling state of photoactive yellow protein. *Biophys. J.* 88:3525–3535.
54. Bernard, C., K. Houben, …, N. A. van Nuland. 2005. The solution structure of a transient photoreceptor intermediate: delta25 photoactive yellow protein. *Structure.* 13:953–962.